Manuscript submitted to **Biophysical** *Journal*

Article

A model for the Hippo pathway in the *Drosophila* wing disc

J. Gou, L. Lin, and H. G. Othmer[1]

[1]School of Mathematics, University of Minnesota, Minneapolis, MN

*Correspondence: othmer@math.umn.edu - J.Gou and L. Lin contributed equally.

ABSTRACT While significant progress has been made toward understanding morphogen-mediated patterning in development, control of the size and shape of tissues via local and global signaling is poorly understood. In particular, little is known about how cell-cell interactions are involved in the control of tissue size. The Hippo pathway in the *Drosophila* wing disc involves cell-cell interactions via cadherins, which leads to modulation of Yorkie, a co-transcriptional factor that affects control of the cell cycle and growth, and studies involving over- and under-expression of components of this pathway reveal conditions that lead to tissue over- or undergrowth. Herein we develop a mathematical model of the Hippo pathway that can qualitatively explain these observations, made in both whole-disc mutants and mutant-clone experiments. We find that a number of non-intuitive experimental results can be explained by subtle changes in the balances between inputs to the Hippo pathway, and suggest some predictions that can be tested experimentally. We also show that certain components of the pathway are polarized at the single cell level, which replicates observations of planar cell polarity. Since the signal transduction and growth control pathways are highly-conserved between *Drosophila* and mammalian systems, the model we formulate can be used as a framework to guide future experimental work on the Hippo pathway in both *Drosophila* and mammalian systems.

INTRODUCTION

The *Drosophila* wing disc (Fig. 1 (a)) is an excellent system for studying the signal transduction and gene control networks involved in growth control, many of which were first discovered there. Growth control in the disc involves both local signals within the disc (1), and system-wide signals such as insulin and insulin-like growth factor that coordinate growth across the organism (2, 3). Both disc-wide and clone experiments with various mutants have led to a rich variety of abnormal growth patterns that remain to be explained in the framework of the known signaling networks, but we will show that these can be understood as the result of subtle alterations in the balances between the outputs of pathways in these networks. Since the pathways are tightly linked, the strengths of the interactions determine the outcome, and thus a Boolean on-off description in terms of activation and inhibition of the components is insufficient – a quantitative model is needed.

The core Hippo pathway or module is a highly-conserved kinase cascade that comprises the kinases Hippo (Hpo) and Warts (Wts) and the adaptor proteins Salvador (Sav) and Mob-as-tumor-suppressor (Mats) (*cf.* Fig. 1 (b)). The key effector of this module is Yorkie (Yki) and Wts is its master regulator. Yki is a co-transcription factor whose nuclear access is controlled by Wts via phosphorylation – phosphorylated Yki (Yki_p) cannot enter the nucleus and thus is transcriptionally inactive. In the nucleus Yki binds to transcription factors such as Scalloped (Sd) to activate the expression of *cyclin E, myc, DIAP1*, and *bantam*, which regulate cell proliferation and apoptosis, and it also controls expression of genes upstream of the Hippo module, such as *expanded, merlin, kibra*, and *four-jointed* (*fj*) (4–9). A number of upstream species regulate the level of Yki by modulating different components of the core Hippo pathway. Among them, Fat (Ft) and Dachsous (Ds) are two atypical cadherins involved in cell-cell interactions that control pathways which lead to direct regulation of Wts (*cf.* Fig. 1 (b)). A number of their mutants and their effect on growth have been identified, but whether the mammalian homologs of Ft and Ds function in the same way as in *Drosophila* is as yet undecided (10). In addition to Ft and Ds, the cell-autonomous CEMK module consisting of Crumbs, Expanded, Merlin and Kibra also affects the Hippo pathway (11) by phosphorylating Hippo, which in turn activates Wts by phosphorylating it at an activation site (12). However, it is less well-characterized and apparently acts independently of the Ft-Ds pathways (13). Therefore, it will not be modeled in detail – we assume throughout that Wts is in the active, phosphorylated form until it is phosphorylated at the inactivation site (14), and focus on the effects of cell-cell interactions.

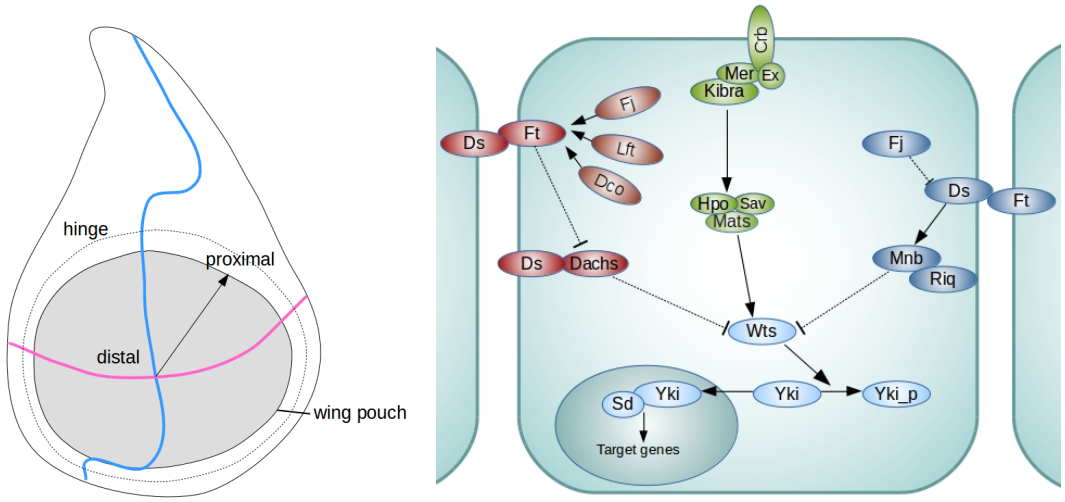

Figure 1: (a) A schematic diagram of the *Drosophila* wing disc. The arrow indicates the direction from distal to proximal. The shaded area denotes the wing pouch and the hinge region is outside the wing pouch and enclosed by the dashed curve. (b) A schematic of the signaling network in contiguous cells. Solid lines denote activation, dashed lines denote inhibition. There are two major Ft/Ds-controlled pathways described in the text– one promoting Yki phosphorylation via Ft inhibition of Dachs membrane-localization and destruction of Wts, and one promoting Yki activity via inactivation of Wts through Riq.

Both Ft and Ds are large cadherins with intracellular, transmembrane and extracellular domains. The intracel-

lular domains (ICDs) of each can independently modulate Yki levels within a cell, while Ft and Ds on adjacent cell membranes can also associate via their extracellular domains (ECDs) to strengthen the signaling and thereby mediate cell-cell interaction(s). This illustrates a central feature of this system – there are cell autonomous effects controlled by the components in the cytoplasm or nucleus and the ICDs of Ft and Ds, as well as non-autonomous effects caused by binding of an ECD of Ft or Ds to the ECD of its heterophilic partner.

Binding between Ds and Ft is modulated by Fj, which phosphorylates the ECDs of Ft and Ds in the Golgi (15). Phosphorylation of Ft enhances its affinity to Ds, while phosphorylation of Ds decreases its affinity for Ft (16). However, the weaker phenotype of *fj* mutants as compared to *ds* mutants and the ability of cells expressing high levels of Ft and Ds to associate without Fj, implies that each has a basal affinity for the other (16).

Ft expression in the disc is quite uniform while Ds and Fj are expressed in a graded manner. Ds expression is low in the wing pouch and is largely confined to the hinge region (17, 18) (Fig. 1 (a)), while Fj is expressed in a decreasing gradient from the disc center to the periphery (19). A recent study suggests that Fj forms a shallow gradient with linear slope of around 3 % between cells along the proximal-distal axis (20). Since *fj* is one of the target genes of Yki, there is an intracellular feedback loop involving Fj that may contribute to cell polarization, as previous studies have suggested (21–23). A number of mathematical models have been developed to study the impact of Ds and Fj gradients on planar polarization (20, 24–26), but the role of gradients of either in growth control is less well understood. Since we focus on growth control, we first ignore polarized expression of Ds and Fj, but later their effects are incorporated.

Signaling from the ICD of Ft suppresses growth via Dachs (Dh), an atypical myosin that is epistatic to *fat* in terms of its growth effect. In normal development Dh accumulates near the adherens junctions, and membrane-localized Dh can bind Wts and promote its degradation (27), thereby reducing the inhibitory effect of Wts on Yki (Fig. 1 (b)). Loss of *dachs* completely suppresses the overgrowth induced by the *fat* loss-of-function mutant, which can be understood from Fig. 1 (b). Overexpression (OE) of *dachs* increases wing size, while wing size decreases in the *dachs* loss-of-function mutant (28). In *ds* mutants, strong but nonpolarized membrane localization of Dh is detected, and in *fat* mutants, there is no detectable change in overall Dh protein levels, which indicates that Ft probably affects the membrane localization of Dh. Experiments suggest that while the polarization of Dh controlled by Ft and Ds is essential for planar cell polarity, it is the amount of Dh localized on the membrane that controls cell growth (28).

Signaling from the ICD of Ds enhances growth by direct interaction with Riquiqui (Riq), a scaffold for protein-protein interactions, and Minibrain (Mnb), a DYRK family kinase (14). Ds is required for localization of Riq at the apical junctions, and localized Riq potentiates Mnb phosphorylation of Wts, which reduces its activity (14). While Ds binding to Ft enhances the inhibitory effect of Ft on Dh localization, the complex also increases binding of Riq to Ds and thereby enhances Riq localization. Recent studies suggest that the Ds ICD and Dh also interact (29), and this may be reinforced in the Ft-Ds complex. However, since modulating the expression of either Riq or Mnb does not influence Dh levels or localization (14), it may be that either Ds ICD has independent binding sites for Riq and Dh, or that Ds only interacts with localized Dh.

Experimental results using disc-wide interventions or mutant clones raise several questions concerning how Ft

and Ds collaborate to regulate the Hippo pathway. For instance, the effect of Ft on growth is not a strictly decreasing function of the Ft level, as might be expected (26). OE of *fat* above wild-type (WT) levels decreases the wing size and complete knockout (KO) of *fat* increases the size, but a knockdown of *fat* decreases, rather than increases, the size. Similarly, the effect of Ds is also non-monotonic: loss of Ds results in enlarged wing discs (30), but OE of Ds using Gal4/UAS – a system for controlling expression of a specified gene by expression of a transcription factor (Gal4) that binds to a specific promoter site (UAS) upstream of that gene – can either reduce (30, 31) or enhance growth (14). In addition, double mutants of *fat* and *ds* overgrow more than either of the single mutants, which suggests that with respect to overgrowth, there is a Ft-independent effect of Ds (32). Growth is also non-monotonic in the expression level of *fj*, and when *fj* and *ds* are co-overexpressed, the reduction in wing size exceeds that of either separately (30, 31).

Similarly puzzling results emerge when mutant clones are used in a WT disc. Clonal OE of *ds* upregulates Hippo target genes in cells on both sides of the border (31, 33), while *ds* loss-of-function clones upregulate Hippo targets outside, but not inside the clone border (33). These require both Ft and Dh, since loss of either suppresses the effects. A similar non-autonomous effect arises when Ft is overexpressed (34, 35), but not when it is underexpressed. Further details are given in recent reviews (36–42), and a summary of experimental observations related to the Hippo pathway is given in Table S3 in the supporting material (SM).

The Hippo pathway functions as the hub of regulatory mechanisms that control growth of the wing disc, and therefore, a mechanistic model of it can provide the framework for integrating other pathways. Most current mathematical models of this pathway focus on planar cell polarity (25, 26, 29, 43–45), while a few touch upon its role in growth (26, 46, 47). However, none describe the Hippo pathway mechanistically, and thus cannot predict how changes in various components are reflected in cellular growth. Herein we develop a mechanistic model that incorporates both the intracellular interactions of some of the principal components in the Hippo pathway and the cell-cell interactions via cadherins at the tissue level. The control mechanisms for tissue growth and size control are complicated and poorly-understood, but it is known that Yorkie is a central factor that reflects changes in the pathways controlled by Ft and Ds, and in turn leads to changes in tissue growth and disc size. Since most of the experimental results related to the Hippo pathway are at the phenotypic level, with little quantitative data available, the purpose of the model is to make qualitative comparisons between model outputs and experimental observations. Throughout we use cytosolic, unphosphorylated Yorkie as a surrogate for cell growth, and denote this by Yki hereafter. If we assume diffusive transport between the cytosol and nucleus, the steady state level of nuclear Yorkie will be proportional to the cytosolic unphosphorylated level.

In the following sections we develop and analyze a mechanistic model that predicts how the level of Yki depends on the effects of cell-cell interactions via Ft and Ds, and on other intracellular reactions. One objective is to provide explanations of some of the seemingly-contradictory experimental results from Ft/Ds mutant experiments described above. The model explains the conflict in the whole-disc observations as the result of the non-monotonic relationship between the Ft and Ds expression levels and the cytosolic Yki level. In addition to the cell-autonomous phenomena, the model shows that several non-autonomous responses can also be explained by the membrane Ft-Ds coupling between neighbouring cells. One example is the boundary effect, in which the downstream effectors of the Hippo

pathway are modulated when neighbouring cells express different amounts of Ds (33). Another is the proliferation of cells adjacent to dead cells. Our model shows that the absence of Ft and Ds in dead cells reduces the amount of Ft-Ds heterodimer on adjacent cells, which in turn enhances repression through Dh, increases active Yki and promotes cell proliferation. Li et al.(48) show the effect of Ft/Ds on the wound-healing process, and Mao et al. (49) show that Dh has an effect on orientated cell division. The effect of Dh on the orientation of cell division reflects its polarization in the disc, and we show that the model reproduces this effect, which is central to planar cell polarity.

METHODS

Most of the existing mathematical models on the Hippo pathway concentrate on the cell polarity, and we are not aware of models that deal with its effect on growth. Given the complexity of the network, we do not incorporate all species and their interactions in the model, but retain only the central components. These are Ft, Ds, Dh, Riq, Wts, and Yki, which are produced constitutively, and complexes between them. Initially we fix the total amount of Fj in all forms, but subsequently investigate the effect of different Fj levels. The signaling network in each cell is shown in Fig. 2 (a). Although there are only 6 primary species, many additional species arise as complexes. All species in the model are listed in Table S1, and the reactions and the equations governing their evolution are given in the SM. A brief summary of the important assumptions underlying the model is given next – a more detailed description of the model and the experimental justification of the assumptions is given in the SM.

- The ECDs and ICDs of Ft and Ds are phosphorylated at several sites, which affects their activity differently. In the model, the phosphorylation of Ft and Ds catalyzed by Fj refers to the ECD, and this modulates the binding between them. Phosphorylation of the ICDs of Ft and Ds is induced by heterodimer formation, which increases their signaling (17, 30). We assume that phosphorylation of the ICDs is fast, which implies that the concentration of the phosphorylated form is proportional to the total concentration of each species.
- The inhibitory effect of Ft on membrane-localization of Dh is modeled by a reduction in the Dh binding rate, and is represented by a decreasing Hill function of Ft and all its complexes. Also, the fact that overgrowth in *fat-ds* double mutants exceeds that of either single mutant indicates a Ft-independent negative regulatory effect of Ds on growth (32). This follows from the fact that in the absence of such an effect Yki would increase as Ds increases due to the positive Ds–Riq effect on Yki, but this is contrary to the result for double mutants. Binding of Dh to the ICD of Ds is observed in *Drosophila* scutellum cells (29), and taken together these facts lead to the hypothesis that localized Dh-Ds complexes decay faster than uncomplexed Dh. This hypothesis ascribes a negative regulatory effect of Ds on growth via degradation of Dh in the complex(4).
- Since Ds is required to recruit Riq to apical junctions, and this is enhanced by Ft-Ds (26), we assume that cytosolic Riq binds directly to either Ds or Ft-Ds on the membrane.

All protein-protein interactions in the model are described by a reversible reaction step for the binding and release of complex partners, and the kinetic rate constants carry appropriate subscripts (See SM). An irreversible catalytic step describes subsequent protein modification, including decay and phosphorylation of Wts. Dephosphorylation steps are included for the phosphorylation of Ft and Ds by Fj. All species X decay via first-order kinetics in the

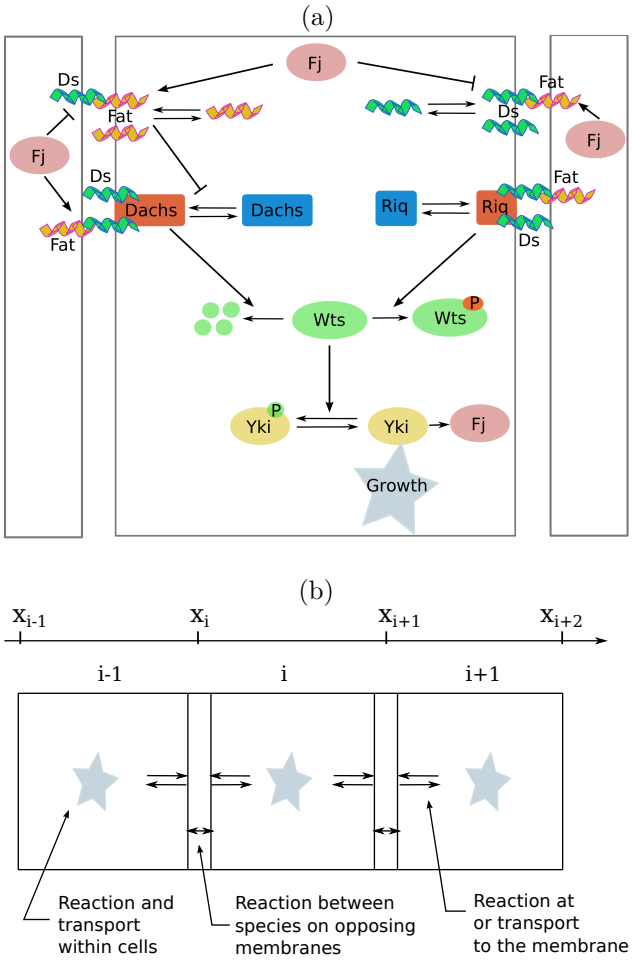

Figure 2: The model diagram. (a): There is a top-level Ft & Ds module, an intermediate Dh & Riq module, and a terminal Wts & Yki module. The Ft-Dh path depresses Yki, while the Riq-Wts pathway enhances the Yki effect on growth. (b): A schematic of a 1D network of coupled cells showing the processes within and between cells. Equations and details are given in the SM.

cytosol, and similarly on the membrane, where decay or turnover of species may result from endocytosis or other degradation mechanisms. The detailed justifications for each reaction are presented in the SM. We consider an array of discrete cells, as indicated schematically in Fig. 2(b), and incorporate reaction and transport steps within each cell, reactions between membrane-bound species and species in the associated cytosol, and reactions between species on two adjacent membranes. The movement of cytosolic species within each cell is modeled by diffusion. The one-dimensional model can be considered as a description of a row of three-dimensional cells in which there is no transverse or apical-basal variation of any species.

Adjacent cells interact through the formation of the heterodimer Ft-Ds. For instance, Ft in the i^{th} cell binds to either membrane of that cell, and membrane-bound Ft binds to Ds on the membrane of the neighboring cell. The left and right cell membranes of the i^{th} cell are labeled as x_i and x_{i+1}, respectively. As the space between

cells is ignored, x_i represents the membrane common to the i^{th} cell and the $(i-1)^{th}$ cell, while x_{i+1} represents the membrane common to the i^{th} cell and the $(i+1)^{th}$ cell, as shown in Fig. 2(b). To label transmembrane Ft-Ds complexes we distinguish left and right membranes of a cell and thus distinguish between Ft-Ds and Ds-Ft complexes on the same membrane.

We divide the Hippo pathway into three modules: the top-level Ft & Ds module, which interacts with neighboring cells and receives intercellular signals; an intermediate Dh & Riq module, whose behavior is controlled by upstream signals and which interacts directly with Wts; and a terminal Wts & Yki module, where Yki is the key output. The Yki output of the third module is the benchmark for comparison with the phenotypes observed in experiments.

In summary, there are 46 variables in the model system and each satisfies a partial or ordinary differential equation. The full system of equations is given in the SM. To solve for the steady state of governing equations, we first discretize the partial differential equations (PDEs) using a standard finite difference method, and solve the large ODE system numerically. We have solved the evolution equations from randomly-chosen initial conditions and find that the steady state is reached in about 3 hours, which is short relative to the cell cycle time. We have also solved the steady state equations directly and neither method shows multiple valid steady states.

Unless stated otherwise, periodic boundary conditions are used, when simulating a one-dimensional array of cells. The number of cells is chosen to be large enough so that any local non-autonomous effects can be captured. In particular, when simulating the effects of mutant cell clones, the size of the system is chosen large enough so that the non-autonomous effect appearing at one clone boundary does not interact with the effect from the other clone boundary.

RESULTS

Numerical values for the kinetic parameters in the model are currently unknown, and therefore we tested parameters within wide biologically-meaningful ranges to understand the sensitivity of the predictions to variations of the parameters. The model parameters are listed in Table S2, and a sensitivity analysis to identify key parameters is discussed in the SM.

The Non-monotonic Response of Yki

Since we first assume that Ds and Fj expression is spatially-uniform in WT discs, all cells in the disc, except perhaps those at the boundaries, behave similarly. Thus the interactions can be understood by analyzing the signaling network in a single cell in which the reciprocal binding of Ft and Ds between cells is incorporated by identifying the two sides of the cell. This reduction provides a tractable way to explore the disc-wide behaviors, including the effect of mutants.

Under this assumption the model reduces to a small system of reaction-diffusion equations with nonlinear boundary conditions that is solved for the steady-state concentrations of all species. The predicted Yki concentration (which is the cytosolic, unphosphorylated level) as a function of the Ft and Ds production rates is shown in the

'heat-map' in Fig. 3. Although details of this map depend on parameters, it has several important features. Firstly, in $ds^{-/-}$ mutants the Yki concentration decreases monotonically with the Ft production rate, since the stimulative effect of the Ds-Riq path is absent. In $ft^{-/-}$ mutants the inhibitory effect of Ft is absent and Yki is regulated by the Ds-Riq pathway and the Dh-Ds interaction. Another prediction is that double mutants of *fat* and *ds* – (0,0) in Fig. 3 – overgrow slightly more than either single mutant. Our computations show that the Yki level in $fat^{-/-}$ and WT Ds is 710 nM, in $ds^{-/-}$ and WT Ft it is 570 nM and in $ft^{-/-}$-$ds^{-/-}$ it is 770 nM. These predictions are in qualitative agreement with experimental results. The double-mutant prediction stems from the fact that there is a Ft-independent negative regulatory effect of Ds on Dh in the model. Previous work has shown that knockout of *ds* potentiates the overgrowth in *ft* mutants, but failed to uncover a mechanistic basis (32). Our explanation is that with or without Ft, membrane-localized Dh is degraded more rapidly when bound to Ds, and therefore in $ds^{-/-}$ mutants the inhibition of Wts by Dh is increased, and Yki increases. A reduced model that lacks the Dh-Ds interaction cannot predict the double-mutant effect, although other effects are predicted (data not shown).

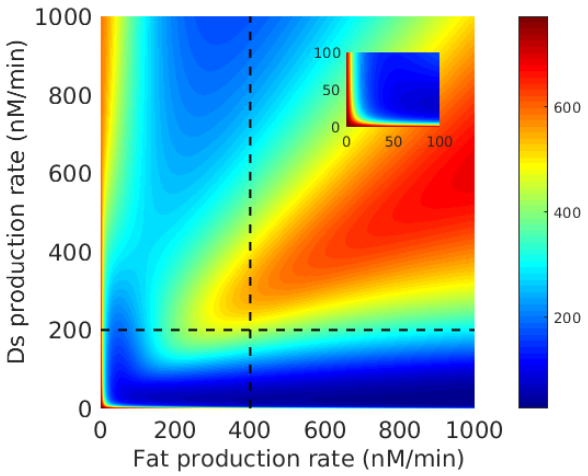

Figure 3: The growth response, as reflected by the Yki concentration, as a function of Ft and Ds production rates. The colorbar indicates the Yki concentration in nanomolar units. WT rates are (Ft,Ds) =(400,200) nM/min. Inset: enlarged heat-map in the range of 0 - 100 nM for both Ft and Ds.

In contrast to the monotonic response of Yki in either a Ft or Ds KO, the response of Yki is non-monotonic when Ds expression is fixed at the WT level and Ft production is varied, or conversely, when Ft expression is at the WT level and Ds is varied, as shown in Fig. 4(a) & (b). Fig. 4(a) shows that a Ft KO causes overgrowth, and sufficiently large OE of Ft causes undergrowth, but in the intermediate range, reduction of Ft production from the WT level first enhances but then reduces growth. This is in qualitative agreement with experimental observations in (26), where a weak effect on wing size was observed in partial *ft* knockdowns. The WT production level of Ft and Ds were set at an intermediate value to account for these observations, and it can be seen in Fig. 3 that other combinations of Ft-Ds production can lead to similar results.

To understand the non-monotonic response, suppose that the Ft production rate is increased from zero, and

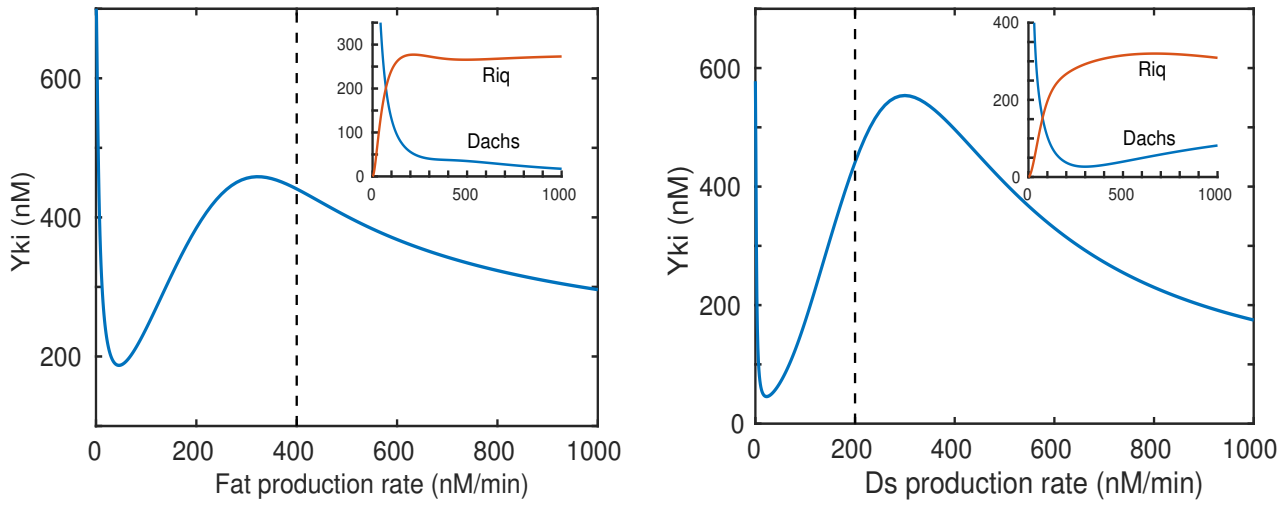

Figure 4: The Yki concentration as a function of the Ft or Ds production rate. Here and hereafter the Yki levels represent an average of the Yki concentration over the cell. (a) A horizontal slice of the growth response map shows non-monotonic dependence of Yki on Ft expression, and vertical slice (b), shows a similar dependence on Ds expression. Insets show the levels of Wts-bound Dh and its complexes, and Wts-bound Riq complexes, both in nM, as a function of Ft production and Ds production, respectively. Both (a) and (b) reflect the fact that the qualitative conclusions concerning the effects of over- and under-expression are relatively insensitive to the choice of WT production levels, i.e., the non-monotonic response of Yki to Ft and Ds production levels is robust.

consider the response of Wts bound to Dh and its complexes *vs.* the response of Wts bound to Riq complexes, as shown in Fig. 4(a-inset). The former decreases rapidly due to increased inhibition of Dh localization, which leads to reduced Wts degradation and decreased Yki. On the other hand, the Wts-Riq complexes increase with Ft production, which leads to an increase in Yki. At low Ft the Wts reduction dominates, but at $\sim$50 nM/min the effects balance, and thereafter Yki increases until the level of Wts-Riq complexes saturates at $\sim$300 nM/min, which sets the second maximum of Yki. Beyond that the residual level of inhibition via the Ft pathway produces a slow decline in Yki. The balance between the pathways is subtle because Ft affects Dh and Riq through distinct mechanisms, and because the inhibitory effects of Ft and Ft-Ds on Dh localization have different strengths.

The model can also explain seemingly contradictory effects of the Ds expression level on growth. Some previous results showed that OE of Ds represses Yki activity (30, 31), but others have argued that it simulates Yki activity (14). Our results suggest that this disparity may stem from the use of different Gal4 drivers in these experiements. The OE level of *ds* induced by *tub-Gal4* or *en-Gal4* observed in (30, 31) may be higher than that induced by *hh-Gal4* used in (14), which can lead to lower or higher than WT Yki levels for suitable choices of Ds expression in Fig. 4(b). A vertical section of Fig. 3 at the WT Ft production rate leads to the Yki *vs.* Ds curve shown in Fig. 4(b). While strong OE of Ds reduces Yki activity and growth, moderate OE – from the WT 200 nM/min to $\sim$ 400 nM/min – increases Yki activity and stimulates growth. Furthermore, the production rate that sets the mid-range maximum growth depends on the Ft production rate. The model also predicts a non-monotonic effect

on growth below WT levels of production – complete loss of Ds causes overgrowth, and partial loss of Ds reduces growth. This is remarkably similar to the observation when Ft function is lost, emphasizing the similarity of the effects of the two atypical cadherins. These predicted effects can easily be tested experimentally.

One also finds that the Yki level is a monotone increasing function of the Dh or Riq production rate (results not shown). As the expression level of Dh increases at a fixed Ft level, its degradation of Wts increases, and as a result Yki activity increases. Similarly, when Riq is overexpressed the regulatory effect of the Riq-Ds pathway is increased, and again Yki increases.

Another interesting phenomenon in the wing disc is cell competition, in which some cells that are more fit by some measure out-compete less fit cells. The former proliferate to compensate for the lost cells, which is similar to apoptosis-induced compensatory proliferation (50). Experiments have shown that cells adjacent to dead cells or 'gaps' undergo cell proliferation, as occurs in wound healing. Also, Ft and Ds are required for orientated cell division under such circumstances (48). In the SM we show that the lack of signals from dead cells is reflected in the altered level of the Ft-Ds heterodimer, which affects the membrane localization of Dh as well as the downstream signaling of the Hippo pathway. To illustrate what the model predicts, we consider a line of 11 cells, five on either side of one that is "dead" in the sense that all membrane-mediated interactions with neighboring cells are removed and its reactions are stopped. Fig. S5 shows that the two cells adjacent to the dead cell have a higher Yki concentration and hence would overgrow. This results from two competing effects, (i) the reduction of the inhibitory effect of the Ft-Dh pathway in the WT neighbors due to the loss of Ft_{WT}-Ds_{D} – where the subscript D refers to the dead cell – binding, and (ii) the reduction of the Riq effect due to the loss of Ft_{D}-Ds_{WT} binding. Here the former dominates, but more experiments are required to confirm this explanation.

The Effect of Fj and Ds Gradients on Planar Cell Polarity

In the previous section we analyzed the Yki levels as a function of the Ft and Ds production rates in a background of a constant level of Fj and uniform expression of Ds. However, as remarked earlier, experimental results show that both Fj and Ds expression levels are graded from distal to proximal in the wing disc, with Fj high at the center of the disc and Ds high at the periphery (17, 19, 21, 51). The role of these gradients in regulating planar cell polarity (PCP) are well-studied (20, 44), and experiments also show that altering the gradients can trigger different effects on growth (31, 33, 52). Thus we next investigate how the level of Yki is affected by the local Fj production and by the Fj/Ds gradients.

In Fig. 5 we show that the unphosphorylated Yki level is reduced for either a Fj knockdown or overexpression, which agrees with the experimental observation that the wing size is reduced in both Fj mutants and OE (30, 31). Because the only role that Fj plays in the model is to phosphorylate Ft and Ds, the Yki profile as a function of Fj depends on the downstream effects of different complexes in the Ft and Riq pathways, and in particular, on the relative level of different Dh and Riq complexes. Because we do not distinguish between the effects of unphosphorylated and phosphorylated forms of the same complex on the downstream signals, the effect of Fj on Yki level stems solely from the redistribution of Dh and Riq complexes when Fj is varied. For instance, when the

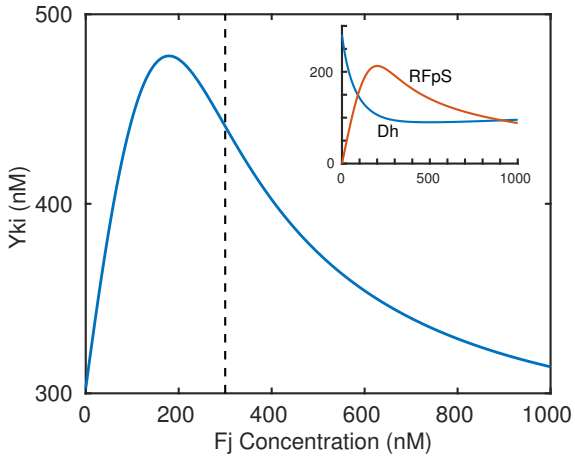

Figure 5: The Yki level as a function of the Fj concentration. The inset shows the variation of free Dh and Riq-Ft$_p$-Ds (RFpS), both in nM, with the Fj concentration.

Fj concentration increases from 0, the existing Dh-Ds complexes are converted to Dh-Ds$_p$ complexes and more Dh-Ft$_p$-Ds and Dh-Ft$_p$-Ds$_p$ complexes are formed. This leads to increased degradation of Wts and increased Yki. In addition, the Riq-Ft$_p$-Ds (RFpS) complex increases as Fj increases (see Fig. 5 inset) and together these account for the increasing phase of Yki with Fj. Beyond a Fj concentration of about 200 nM the Dh level and its complexes saturate, while the RFpS level decreases, which accounts for the decreasing phase in Fig. 5.

Next we examine the effect of Fj and Ds gradients. Consider a line of cells, which can be thought of as a radial, distal-proximal slice of the disc, in which the Ds (Fj) production rate increases (decreases) linearly from left to right (Fig. 6). Experiments (31, 53) show that the Ds level is modestly graded from distal to proximal, and we use a slowly-increasing function to represent its distribution.

The model predicts both an increasing Yki profile in the cell array (data not shown), and the polarization of Dh across individual cells in the array, as shown in Fig. 6. The positive values indicate the preferred distal localization of Dh, as observed in experiments (28) and shown in the inset. Furthermore, the difference ratio increases from left (distal) to right (proximal), which indicates that the polarization of Dh is more significant in the proximal region, also as is observed experimentally (19, 54). These results are in qualitative agreement with experimental observations which show that Dh has an effect on PCP and orientated cell division (49). Both gradients promote this asymmetrical localization of Dh: higher Fj in the 'distal' cell of a pair leads to increased formation of Ft$_p$-Ds and decreased Ft-Ds$_p$ at their common membrane, compared with its 'proximal' neighbor. As a result, the reduced inhibitory effect of the Ft-Ds$_p$ on localization of Dh in the proximal cell leads to increased Dh localization at the distal membrane of that cell. Similarly, a lower level of Ds in the distal cell recruits less Ft to the distal membrane of the proximal cell, which also facilitates the polarized localization of Dh on the distal membrane of a cell.

We also observed asymmetrical subcellular localizations of membrane-bound Ft and Ds in a background Fj gradient, in accordance with the findings in (20). The asymmetry level depends on the location of the cell in a cell array as well as the Fj expression level (results not shown).

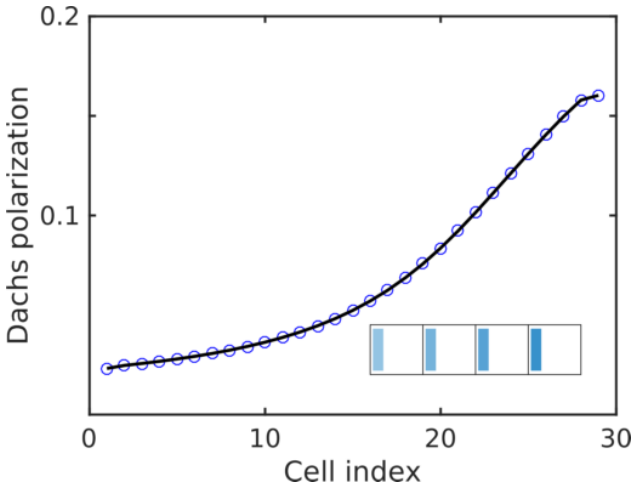

Figure 6: The subcellular localization of Dh calculated from the model under opposing Ds and Fj gradients. From left (distal) to right (proximal), the Ds production increases linearly from 150 nM/min to 200 nM/min and the Fj concentration decreases from 600 nM to 100 nM. Shown is the difference in Dh concentration at the left membrane minus that at the right, divided by the concentration at the left. The inset illustrates the polarization of Dh, which is high at the distal side of cells.

NON-AUTONOMOUS RESPONSES DUE TO CLONES

Both Ft and Ds signal autonomously through the Hippo pathway via their ICDs, but they also modulate cell-cell interactions via their ECDs, and we focus on the latter next. Non-autonomous responses – phenotypes induced in wild-type cells by mutant cells – have been observed in a variety of experiments when Ft/Ds signaling is altered by a mutant clone in a WT disc. For instance, OE of Ds in a clone induces hyperactivity of Yki and OE of target genes on both sides of the interface, and the effect vanishes far from the boundary (33). Fig. 7(a) shows that the model replicates both the elevated level of Yki in both cells at the boundary of the clone and the decay of the effect away from the boundary. Fig. 7(b) shows how localized Dh and Riq are altered in the clone and the adjacent WT cells, and one sees that Dh is highly polarized in the cells near the boundary, while Riq is less polarized. The elevated Yki level near the boundary in Fig. 7(a) is the result of the balance between the inhibitory Ft-Dh pathway and the stimulative Riq pathway. In cell 8 of the clone the Dh level on the membrane adjacent to the WT cell 7 is more than 1.5-fold of the WT, which produces strong inhibition of Wts. Moreover, the localized Riq in clone cells does not vary much and the overall effect explains the increased Yki level in that cell. One also sees in Fig. 7(b) that the Riq level in the interior of the clone is significantly higher than in WT cells, and Dh is significantly lower, but the balance between the positive and negative effects of these pathways leads to a Yki level in the interior of the clone comparable to that in WT cells.

The increases in Yki in the two WT cells closest to the clone are at a level that may not be experimentally detectable, but the results in Fig. 7 ignore changes to the boundary that may arise from the juxtaposition of unlike cell types. For instance, Dh polarization increases junction tension at the border of a clone (4, 29, 55) and

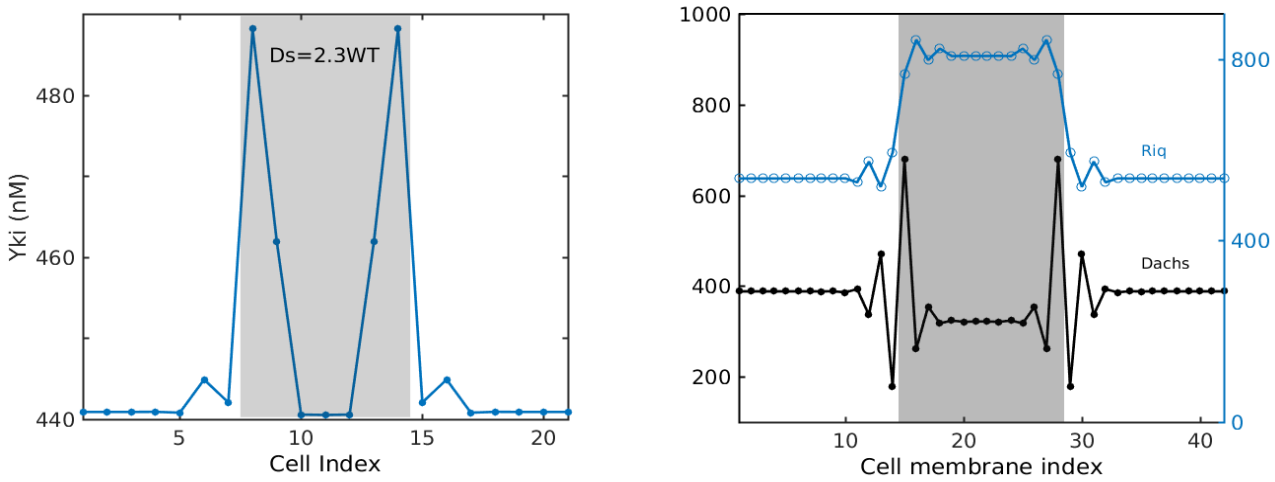

Figure 7: The results of simulating a circular array of 21 cells with a patch of 7 clone cells in the shaded region. (a): The predicted autonomous and non-autonomous Yki concentration induced by 2.3 x WT OE of Ds in the clone. The cell index refers to 21 cells with 7 clone cells shaded. (b): The level of membrane-localized Dh and Riq, in nM, under Ds OE in a clone. The cell membrane index refers to the corresponding 42 locations of cell membranes from 21 cells with 14 locations from 7 clone cells shaded.

it is known that the Hippo pathway responds to mechanical signals (56–58). It is plausible that changing the mechanical properties of boundary cells can affect the interactions of Ft and Ds and result in significant changes in the downstream pathways. If, for example, we reduce the inhibitory effect of Ft-complexes on Dh localization slightly, the boundary effect on the WT side becomes more significant, as shown in Fig. 8.

The cell-cell interactions that arise from the formation of Ft-Ds complexes can also explain other experimental observations. For example, when Ds is knoocked out in clone cells, qualitative analysis of the interactions in the network suggests that a WT cell adjacent to a clone cell will have elevated Yki levels due to the reduced membrane-bound Ft_{WT}-Ds_{C} complex. In contrast, the Yki level at the clone side of the interface is suppressed, as shown in Fig. S6(a). This prediction agrees well with experimental results in which the boundary effect, as reflected in the elevation of the Yki level only appears at one side of the interface in Ds knockout clones (33). We also studied the interaction between WT and clone cells with Ft underexpression in the clone to determine how the level of localized Dh at the interface changes. As shown in Fig. S6(b), Dh accumulates at the clone boundary due to the reduced inhibition of Ft on Dh binding in the clone, which is expected and is as observed in experiments (55).

The model also predicts that the non-autonomous responses at the boundary of a clone would disappear in $fat^{-/-}$, $ds^{-/-}$, or double mutants, as is observed in experiments (33, 35). In particular, in a $ds^{-/-}$ mutant background, OE of Ds induces the boundary effect only in the Ds-expressing cells (33). Other qualitative effects can be predicted, and the model provides a framework for developing experimental tests of such predictions.

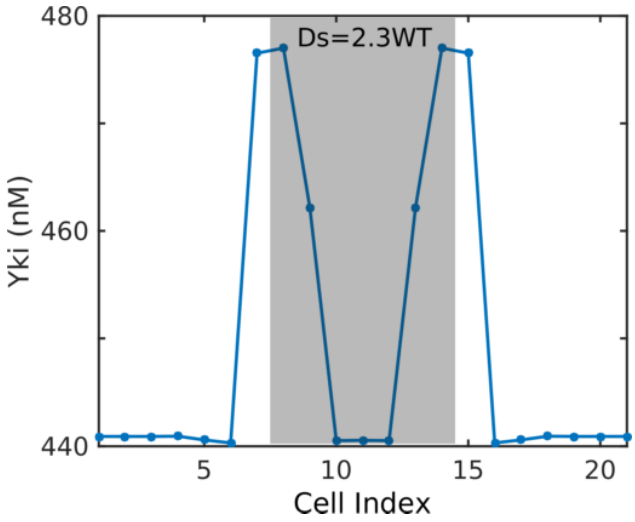

Figure 8: The effect of reducing the inhibition of Ft-Ds complex on Dh localization in the WT cells in contact with clone cells. Other conditions are as in Fig. 7.

DISCUSSION

The goal of this work was to provide a framework for understanding the complex phenotypes associated with the Hippo pathway and to make testable predictions that can guide further experimental studies. The model developed here can replicate all major experimental observations, such as the non-monotonic effects in disc-wide alterations of Ft and Ds expression, and the non-autonomous effects induced by cell clones. The model suggests that the seemingly inexplicable observations derive from the perturbation of the delicate balance between positive and negative control of intra- and intercellular signals. In particular, we showed that the regulation of Dh and Riq localization on the membrane plays a central role in both non-monotonic and non-autonomous effects. The model also predicts a difference between the autonomous and non-autonomous responses stimulated by clone cells with disrupted Ft/Ds signaling, and provides a mechanistic explanation for the *ft*, *ds* double-mutant phenotype, which supports our hypothesis that Ds interacts with Dh. The fact that the model predicts all the major characteristic phenotypes demonstrates the applicability of the model to the Hippo pathway. Though experimental values of parameters are not available, qualitative analysis of the model can lead to an understanding of various experimental results and to predictions of experimentally-testable phenomena.

The non-monotonic response of Ft on growth and the non-autonomous response induced by OE of Ds in cell clones has also been explained by a recent model that assumes mutual inhibition between the opposite orientations of the heterodimers and self-promotion of the same orientations (26). While this is an interesting hypothesis, there is little experimental evidence in support of it. In contrast, the model developed herein does not assume such roles, and yet predicts both the non-monotonic and non-autonomous responses. These stem from the balances between the positive regulatory step from Ds via Riq, and the interactions between Ds and Dh, the latter found *in vitro* (4), but not yet conformed *in vivo*.

While all the major experimental observations can be explained in the one dimensional model developed here, there are a number of directions in which the model and our analysis can be extended. Firstly, the growth of the wing disc is affected by a number of other signaling pathways that affect cell growth, proliferation and apoptosis. These include the Dpp pathway, which functions by repressing the growth repressor *brinker*, as well as JNK, and Stat signaling(59), some of which act independently of Yki, and others of which affect the Hippo pathway. Another aspect that warrants further study is the effect of mechanical stress on tissue size. As discussed earlier, stress can affect junctional tension and single cell growth, but whether it plays a significant role in growth control at the tissue level remains unclear. Theoretical models that predict a significant effect have been formulated (47, 56, 60, 61), and some experimental results suggest an effect of tension on Hippo signaling and growth (62). However, a recent study shows that eliminating the basement membrane, which alters tension throughout the disc, has no effect on the final wing size (63). A more detailed two- or three-dimensional model that incorporates the cytoskeletal structure at the single cell level, the cell-cell interactions via Ft, Ds and other cadherins, and the signaling pathways to Yki, will facilitate theoretical studies of how mechanics and signaling interact.

At present there is no agreed-upon mechanism for size control in organ growth in Drosophila or other systems. Certainly there are system-wide effects, but how might a local control mechanism that acts in concert with the global control function? Given the number and complexity of pathways involved in local control, the mechanism must lie far downstream and must integrate the signals from them to determine when to stop growth. mTOR (mechanistic target of rapomycin) is a potential hub for integrating signaling pathways for nutrients, growth factors, and signaling from other pathways such as the Hippo pathway (64), and could lead to expression of what we call a consensus molecule. One mechanism by which such a molecule might function is as follows.

Suppose that all growing cells produce a molecule C at a constant rate in the tissue $\mathbf{\Omega}$, and that this molecule diffuses throughout the tissue. Further suppose that C is degraded at the boundary. If growth is slow compared to the diffusion of C, C satisfies

$$\frac{\partial C}{\partial t} = D\nabla^2 C + R \qquad\qquad C = 0 \quad on \quad \partial\mathbf{\Omega}$$

If we assume that C equilibrates rapidly on the time scale of tissue growth, then the steady state solution for C is

$$C(\xi) = \frac{L^2 R}{D}\int_{\Omega} G(\xi - \zeta) d\mathbf{\Omega}.$$

where the kernel G reflects the geometry of the tissue. The maximum level of C reflects the size of the tissue, and when the domain is small the maximum of C in the tissue will be small. Since the peak level of C changes with the system size this could provide a mechanism for controlling the size of a tissue, because when the threshold is reached at an interior point a signal to terminate division could be propagated throughout the entire tissue. Of course this is a simplistic description, but it may serve to provoke new ideas as to how a disc knows how big it should be.

AUTHOR CONTRIBUTIONS

L.L. and H.G.O. conceived the original idea and designed the model. J.G. and L.L. performed the numerical simulations. J.G., L.L. and H.G.O. analyzed the data and wrote the manuscript.

ACKNOWLEDGMENT

Supported in part by NIH Grant # GM29123.

SUPPORTING CITATIONS

References (65–74) appear in the Supporting Material.

SUPPORTING MATERIAL

S1 Text

S1 Text provides extended analysis of the model and the parameter estimation schemes. The full set of equations and parameters used in simulations are also included in the supporting material. The code for the simulations is available upon request.

REFERENCES

1. Hariharan, I. K., 2015. Organ size control: lessons from Drosophila. *Developmental cell* 34:255–265.

2. Katsuyama, T., F. Comoglio, M. Seimiya, E. Cabuy, and R. Paro, 2015. During Drosophila disc regeneration, JAK/STAT coordinates cell proliferation with Dilp8-mediated developmental delay. *Proceedings of the National Academy of Sciences* 112:E2327–E2336.

3. Jaszczak, J. S., J. B. Wolpe, R. Bhandari, R. G. Jaszczak, and A. Halme, 2016. Growth coordination during Drosophila melanogaster imaginal disc regeneration is mediated by signaling through the relaxin receptor Lgr3 in the prothoracic gland. *Genetics* 204:703–709.

4. Blair, S., and H. McNeill, 2018. Big roles for Fat cadherins. *Current opinion in cell biology* 51:73–80.

5. Fulford, A., N. Tapon, and P. S. Ribeiro, 2018. Upstairs, downstairs: spatial regulation of Hippo signalling. *Current opinion in cell biology* 51:22–32.

6. Fu, V., S. W. Plouffe, and K.-L. Guan, 2017. The Hippo pathway in organ development, homeostasis, and regeneration. *Current opinion in cell biology* 49:99–107.

7. Meng, Z., T. Moroishi, and K.-L. Guan, 2016. Mechanisms of Hippo pathway regulation. *Genes & development* 30:1–17.

8. Yu, F.-X., B. Zhao, and K.-L. Guan, 2015. Hippo pathway in organ size control, tissue homeostasis, and cancer. *Cell* 163:811–828.

9. Harvey, K. F., and I. K. Hariharan, 2012. The Hippo pathway. *Cold Spring Harbor Perspectives in Biology* 4:a011288.

10. Sun, S., and K. D. Irvine, 2016. Cellular organization and cytoskeletal regulation of the Hippo signaling network. *Trends in cell biology* 26:694–704.

11. Su, T., M. Z. Ludwig, J. Xu, and R. G. Fehon, 2017. Kibra and Merlin Activate the Hippo Pathway Spatially Distinct from and Independent of Expanded. *Developmental Cell* 40:478–490.

12. Sun, S., B. Reddy, and K. D. Irvine, 2015. Localization of Hippo signalling complexes and Warts activation in vivo. *Nature communications* 6:8402.

13. Vrabioiu, A. M., and G. Struhl, 2015. Fat/Dachsous signaling promotes Drosophila wing growth by regulating the conformational state of the NDR kinase Warts. *Developmental cell* 35:737–749.

14. Degoutin, J. L., C. C. Milton, E. Yu, M. Tipping, F. Bosveld, L. Yang, Y. Bellaiche, A. Veraksa, and K. F. Harvey, 2013. Riquiqui and Minibrain are regulators of the Hippo pathway downstream of Dachsous. *Nature Cell Biology* 15:1176–1185.

15. Ishikawa, H. O., H. Takeuchi, R. S. Haltiwanger, and K. D. Irvine, 2008. Four-jointed is a Golgi kinase that phosphorylates a subset of cadherin domains. *Science* 321:401–404.

16. Simon, M. A., A. Xu, H. O. Ishikawa, and K. D. Irvine, 2010. Modulation of fat: dachsous binding by the cadherin domain kinase four-jointed. *Current Biology* 20:811–817.

17. Ambegaonkar, A. A., G. Pan, M. Mani, Y. Feng, and K. D. Irvine, 2012. Propagation of Dachsous-Fat planar cell polarity. *Current Biology* 22:1302–1308.

18. Strutt, H., and D. Strutt, 2002. Nonautonomous planar polarity patterning in Drosophila: dishevelled-independent functions of frizzled. *Developmental cell* 3:851–863.

19. Brittle, A., C. Thomas, and D. Strutt, 2012. Planar polarity specification through asymmetric subcellular localization of Fat and Dachsous. *Current Biology* 22:907–914.

20. Hale, R., A. L. Brittle, K. H. Fisher, N. A. Monk, and D. Strutt, 2015. Cellular interpretation of the long-range gradient of Four-jointed activity in the Drosophila wing. *Elife* 4:e05789.

21. Ma, D., C.-h. Yang, H. McNeill, M. A. Simon, and J. D. Axelrod, 2003. Fidelity in planar cell polarity signalling. *Nature* 421:543–547.

22. Collu, G. M., and M. Mlodzik, 2015. Planar polarity: Converting a morphogen gradient into cellular polarity. *Current Biology* 25:R372–R374.

23. Aw, W. Y., and D. Devenport, 2017. Planar cell polarity: global inputs establishing cellular asymmetry. *Current opinion in cell biology* 44:110–116.

24. Wortman, J. C., M. Nahmad, P. C. Zhang, A. D. Lander, and C. Y. Clare, 2017. Expanding signaling-molecule wavefront model of cell polarization in the Drosophila wing primordium. *PLoS Computational Biology* 13:e1005610.

25. Jolly, M. K., M. S. Rizvi, A. Kumar, and P. Sinha, 2014. Mathematical modeling of sub-cellular asymmetry of fat-dachsous heterodimer for generation of planar cell polarity. *PloS one* 9:e97641.

26. Mani, M., S. Goyal, K. D. Irvine, and B. I. Shraiman, 2013. Collective polarization model for gradient sensing via Dachsous-Fat intercellular signaling. *Proceedings of the National Academy of Sciences* 110:20420–20425.

27. Cho, E., Y. Feng, C. Rauskolb, S. Maitra, R. Fehon, and K. D. Irvine, 2006. Delineation of a Fat tumor suppressor pathway. *Nature Genetics* 38:1142–1150.

28. Mao, Y., C. Rauskolb, E. Cho, W.-L. Hu, H. Hayter, G. Minihan, F. N. Katz, and K. D. Irvine, 2006. Dachs: an unconventional myosin that functions downstream of Fat to regulate growth, affinity and gene expression in Drosophila. *Development* 133:2539–2551.

29. Bosveld, F., I. Bonnet, B. Guirao, S. Tlili, Z. Wang, A. Petitalot, R. Marchand, P.-L. Bardet, P. Marcq, F. Graner, et al., 2012. Mechanical control of morphogenesis by Fat/Dachsous/Four-jointed planar cell polarity pathway. *Science* 336:724–727.

30. Feng, Y., and K. D. Irvine, 2009. Processing and phosphorylation of the Fat receptor. *Proceedings of the National Academy of Sciences* 106:11989–11994.

31. Rogulja, D., C. Rauskolb, and K. D. Irvine, 2008. Morphogen control of wing growth through the Fat signaling pathway. *Developmental cell* 15:309–321.

32. Matakatsu, H., and S. S. Blair, 2006. Separating the adhesive and signaling functions of the Fat and Dachsous protocadherins. *Development* 133:2315–2324.

33. Willecke, M., F. Hamaratoglu, L. Sansores-Garcia, C. Tao, and G. Halder, 2008. Boundaries of Dachsous Cadherin activity modulate the Hippo signaling pathway to induce cell proliferation. *Proceedings of the National Academy of Sciences* 105:14897–14902.

34. Bosch, J. A., T. M. Sumabat, Y. Hafezi, B. J. Pellock, K. D. Gandhi, and I. K. Hariharan, 2014. The Drosophila F-box protein Fbxl7 binds to the protocadherin Fat and regulates Dachs localization and Hippo signaling. *Elife* 3:e03383.

35. Matakatsu, H., and S. S. Blair, 2012. Separating planar cell polarity and Hippo pathway activities of the protocadherins Fat and Dachsous. *Development* 139:1498–1508.

36. Sopko, R., and H. McNeill, 2009. The skinny on Fat: an enormous cadherin that regulates cell adhesion, tissue growth, and planar cell polarity. *Current opinion in cell biology* 21:717–723.

37. Enderle, L., and H. McNeill, 2013. Hippo Gains Weight: Added Insights and Complexity to Pathway Control. *Science signaling* 6:re7.

38. Lawrence, P. A., G. Struhl, and J. Casal, 2008. Do the protocadherins Fat and Dachsous link up to determine both planar cell polarity and the dimensions of organs? *Nature Cell Biology* 10:1379–1382.

39. Halder, G., and R. L. Johnson, 2011. Hippo signaling: growth control and beyond. *Development* 138:9–22.

40. Harvey, K. F., X. Zhang, and D. M. Thomas, 2013. The Hippo pathway and human cancer. *Nature Reviews Cancer* 13:246–257.

41. Staley, B. K., and K. D. Irvine, 2012. Hippo signaling in Drosophila: recent advances and insights. *Developmental Dynamics* 241:3–15.

42. Grusche, F. A., H. E. Richardson, and K. F. Harvey, 2010. Upstream regulation of the Hippo size control pathway. *Current Biology* 20:R574–R582.

43. Amonlirdviman, K., N. A. Khare, D. R. Tree, W.-S. Chen, J. D. Axelrod, and C. J. Tomlin, 2005. Mathematical modeling of planar cell polarity to understand domineering nonautonomy. *Science* 307:423–426.

44. Matis, M., and J. D. Axelrod, 2013. Regulation of PCP by the Fat signaling pathway. *Genes & development* 27:2207–2220.

45. Ma, D., K. Amonlirdviman, R. L. Raffard, A. Abate, C. J. Tomlin, and J. D. Axelrod, 2008. Cell packing influences planar cell polarity signaling. *Proceedings of the National Academy of Sciences* 105:18800–18805.

46. Zecca, M., and G. Struhl, 2010. A feed-forward circuit linking wingless, fat-dachsous signaling, and the warts-Hippo pathway to Drosophila wing growth. *PLoS Biology* 8:e1000386.

47. Aegerter-Wilmsen, T., M. B. Heimlicher, A. C. Smith, P. B. de Reuille, R. S. Smith, C. M. Aegerter, and K. Basler, 2012. Integrating force-sensing and signaling pathways in a model for the regulation of wing imaginal disc size. *Development* 139:3221–3231.

48. Li, W., A. Kale, and N. E. Baker, 2009. Oriented cell division as a response to cell death and cell competition. *Current biology* 19:1821–1826.

49. Mao, Y., A. L. Tournier, P. A. Bates, J. E. Gale, N. Tapon, and B. J. Thompson, 2011. Planar polarization of the atypical myosin Dachs orients cell divisions in Drosophila. *Genes & Development* 25:131–136.

50. Fan, Y., and A. Bergmann, 2008. Apoptosis-induced compensatory proliferation. The Cell is dead. Long live the Cell! *Trends in cell biology* 18:467–473.

51. Yang, C.-h., J. D. Axelrod, and M. A. Simon, 2002. Regulation of Frizzled by fat-like cadherins during planar polarity signaling in the Drosophila compound eye. *Cell* 108:675–688.

52. Brittle, A. L., A. Repiso, J. Casal, P. A. Lawrence, and D. Strutt, 2010. Four-jointed modulates growth and planar polarity by reducing the affinity of Dachsous for Fat. *Current Biology* 20:803–810.

53. Rodríguez, I., 2004. The dachsous gene, a member of the cadherin family, is required for Wg-dependent pattern formation in the Drosophila wing disc. *Development* 131:3195–3206.

54. Merkel, M., A. Sagner, F. S. Gruber, R. Etournay, C. Blasse, E. Myers, S. Eaton, and F. Jülicher, 2014. The balance of prickle/spiny-legs isoforms controls the amount of coupling between core and fat PCP systems. *Current Biology* 24:2111–2123.

55. Bosveld, F., B. Guirao, Z. Wang, M. Rivière, I. Bonnet, F. Graner, and Y. Bellaïche, 2016. Modulation of junction tension by tumor suppressors and proto-oncogenes regulates cell-cell contacts. *Development* 143:623–634.

56. Shraiman, B. I., 2005. Mechanicall feedback as a possible regulator of tissue growth. *Proc. Nat. Acad. Sci.* 102:3318–3323.

57. Aragona, M., T. Panciera, A. Manfrin, S. Giulitti, F. Michielin, N. Elvassore, S. Dupont, and S. Piccolo, 2013. A mechanical checkpoint controls multicellular growth through YAP/TAZ regulation by actin-processing factors. *Cell* 154:1047–1059.

58. Tsoumpekos, G., L. Nemetschke, and E. Knust, 2018. Drosophila Big bang regulates the apical cytocortex and wing growth through junctional tension. *J Cell Biol* jcb–201705104.

59. Atkins, M., D. Potier, L. Romanelli, J. Jacobs, J. Mach, F. Hamaratoglu, S. Aerts, and G. Halder, 2016. An ectopic network of transcription factors regulated by hippo signaling drives growth and invasion of a malignant tumor model. *Current Biology* 26:2101–2113.

60. Aegerter-Wilmsen, T., C. M. Aegerter, E. Hafen, and K. Basler, 2007. Model for the regulation of size in the wing imaginal disc of *Drosophila*. *Mechanisms of development* 124:318–326. Epub 2006 Dec 29.

61. Irvine, K. D., and B. I. Shraiman, 2017. Mechanical control of growth: ideas, facts and challenges. *Development* 144:4238–4248.

62. Pan, Y., I. Heemskerk, C. Ibar, B. I. Shraiman, and K. D. Irvine, 2016. Differential growth triggers mechanical feedback that elevates Hippo signaling. *Proceedings of the National Academy of Sciences* 201615012.

63. Ma, M., X. Cao, J. Dai, and J. C. Pastor-Pareja, 2017. Basement membrane manipulation in Drosophila wing discs affects Dpp retention but not growth mechanoregulation. *Developmental cell* 42:97–106.

64. Saxton, R. A., and D. M. Sabatini, 2017. mTOR signaling in growth, metabolism, and disease. *Cell* 168:960–976.

65. Pan, G., Y. Feng, A. A. Ambegaonkar, G. Sun, M. Huff, C. Rauskolb, and K. D. Irvine, 2013. Signal transduction by the Fat cytoplasmic domain. *Development* 140:831–842.

66. Willecke, M., F. Hamaratoglu, M. Kango-Singh, R. Udan, C. lin Chen, C. Tao, X. Zhang, and G. Halder, 2006. The fat cadherin acts through the Hippo tumor-suppressor pathway to regulate tissue size. *Current Biology* 16:2090–2100.

67. Feng, Y., and K. D. Irvine, 2007. Fat and expanded act in parallel to regulate growth through warts. *Proceedings of the National Academy of Sciences* 104:20362–20367.

68. Badouel, C., L. Gardano, N. Amin, A. Garg, R. Rosenfeld, T. Le Bihan, and H. McNeill, 2009. The FERM-domain protein Expanded regulates Hippo pathway activity via direct interactions with the transcriptional activator Yorkie. *Developmental cell* 16:411–420.

69. Hamaratoglu, F., M. Willecke, M. Kango-Singh, R. Nolo, E. Hyun, C. Tao, H. Jafar-Nejad, and G. Halder, 2005. The tumour-suppressor genes NF2/Merlin and Expanded act through Hippo signalling to regulate cell proliferation and apoptosis. *Nature cell biology* 8:27–36.

70. Saltelli, A., M. Ratto, T. Andres, F. Campolongo, J. Cariboni, D. Gatelli, M. Saisana, and S. Tarantola, 2008. Global sensitivity analysis: the primer. John Wiley & Sons.

71. Lin, L., and H. G. Othmer, 2017. Improving Parameter Inference from FRAP Data: an Analysis Motivated by Pattern Formation in the Drosophila Wing Disc. *Bulletin of mathematical biology* 79:448–497.

72. Saltelli, A., P. Annoni, I. Azzini, F. Campolongo, M. Ratto, and S. Tarantola, 2010. Variance based sensitivity analysis of model output. Design and estimator for the total sensitivity index. *Computer Physics Communications* 181:259–270.

73. Garoia, F., D. Guerra, M. C. Pezzoli, A. López-Varea, S. Cavicchi, and A. Garcı&a-Bellido, 2000. Cell behaviour of Drosophila fat cadherin mutations in wing development. *Mechanisms of development* 94:95–109.

74. Johnston, L. A., and P. Gallant, 2002. Control of growth and organ size in Drosophila. *Bioessays* 24:54–64.